Modelling the Kinetics of Elements Release from a Zeolitic-Rich Tuff

Eleonora Grilli [1], **Antonio Ganga** [2] and **Stefano Salvestrini** [1,3,*]

[1] Department of Environmental, Biological and Pharmaceutical Sciences and Technologies, University of Campania "Luigi Vanvitelli", via Vivaldi 43, 81100 Caserta, Italy; grillieleonora@hotmail.it

[2] Department of Architecture, Design and Urban Planning, University of Sassari, Polo Bionaturalistico, Via Piandanna n° 4, 07100 Sassari, Italy; anto.ganga@gmail.com

[3] Environmental Technologies, University Spin-Off of University of Campania "Luigi Vanvitelli", via Vivaldi 43, 81100 Caserta, Italy

* Correspondence: stefano.salvestrini@unicampania.it; Tel.: +39-0823-274-639; Fax: +39-0823-274-605

check for updates

Abstract: The present investigation aims at modeling the kinetics of elements (Fe, Mg, K, Ca, Na, Al, and Si) release from zeolitic-rich Phlegraean Yellow Tuff weathered by tannic acid solutions at different concentration. Three equations were tested—power function, the Weber–Morris model, and the Elovich equation. Power function was revealed to be an excellent empirical equation well fitted to the experimental data. Its numerical parameters were suitable predictive tools, highlighting both the intensity and modality of weathering processes. By paralleling the dissolution rates, it was possible to allow rock-sources from which elements were released during three distinct weathering stages—(i) the first stage was dominated by biotite and amorphous weathering, (ii) the second stage also started with the breakdown of zeolite framework; and (iii) in the third stage, the whole of weathering/release process approached a steady state. Finally, these outcomes may be used to forecast the pedogenic/nutritional potential of zeolitic-rich tuffs as pedotechnical matrices in restoration design.

Keywords: zeolitic-rich tuff; weathering; kinetic models; power function; elements release rate; tannic acid

1. Introduction

Natural zeolites, or, more precisely, natural zeolite-bearing rocks such as zeolitic-rich tuffs, have been widely utilized in various fields pertaining agro-environmental topics [1–8], from the increasing of soil fertility *lato sensu* to the cleaning of contaminated sites [9–16]. A novel, interdisciplinary field of zeolites application deals with pedotechnologies [17–26], i.e., a specific branch of soil science devoted to improve or even ex novo restoring the whole soil functions [27,28]. Indeed, as natural rocks, zeolitic-rich tuffs undergo pedogenization, viz. an ensemble of weathering + alteration + transformation + evolution processes, which leads to soil formation. It is evident that weathering is the opening driving-force from which the other processes originate. As a matter of fact, even when soil is developed, all the earlier soil-forming processes still operate by reaching a sort of a self-adjusting equilibrium.

On the other hand, the rate of pedogenization depends on the contribution of various factors, such as time, climate, parent material, geomorphology, and organisms. The chemical-mineralogical features of soil formed in the course of pedogenesis are almost governed by the nature of rock parent material. In particular, as volcanic rocks, zeolitic-rich tuffs provide soil with both amorphous and crystalline phases, which variously support the overall soil fertility, e.g., by increasing water retention, cation exchange capacity (CEC), and potassium (a fundamental plant nutrient, along with nitrogen

and phosphorus) availability to plants [29]. Thanks to these (and other) positive traits, zeolitic-rich tuffs have been proposed as "pedotechnomaterials" to be added to soil or to be utilized as such to improve the performance of degraded soils, or to rebuild lost/ablated soils. Consistently with the remarks above, zeolitic-rich tuffs are added as "embryonic" material from which an "anthropogenic" soil is expected to evolve.

However, studies until now progressed in this field only consider the effects of zeolitic-rich tuffs addition from the quantitative standpoint. Actually, it appears important to study and elucidate the evolution of the "embryonic soil" from the qualitative point of view, especially to investigate "if" and "how" the expected phenomena occur and, possibly, to pattern the observed events. Such an investigation is obviously relevant for applied studies, i.e., to check and evaluate the efficiency of pedotechnical interventions, as well as in basic pedology studies, to understand and better clarify the soil forming processes, with special reference to weathering [18,30,31]. An adequate approach to such studies is to transfer the complexity and the huge dimension of natural event to laboratory-scale models; this choice allows us to (i) obtain reliable results within time-limits shorter than the naturals, (ii) avoid the possible environmental interferences, and (iii) discriminate the peculiar effects due to each component of the model. Furthermore, the use of laboratory models makes the application and comparison of equations fitting experimental results easy and consistent [32].

A convenient way to analyze rock weathering processes using laboratory models is to subject them to periodical solution replacement, simulating the natural occurrence of rainfall (irrigation)/leaching [30]. Following this approach, a previous work studied the elements release from Phlegraean Yellow Tuff weathered by water and tannic acid solutions (TA) at different concentration, ranging from 3×10^1 to 3×10^4 μmol·L^{-1}, during a 161 days lab scale experiment. Two main results were acquired:

(i)　the weathering effectiveness of the different solutions is quite proportional to the order of exponential magnitude of the TA concentration, viz. $0 < n \times 10^1$ μmol·L$^{-1} \cong n \times 10^2$ μmol·L$^{-1} < n \times 10^3$ μmol·L$^{-1} < n \times 10^4$ μmol·L^{-1};

(ii)　the variability of electrical conductivity and proton budget activity of rock/solutions, as well as the elements release seem to be differentiated in three distinct temporal stages, probably due to the weathering of different mineralogical phases over time.

These findings also suggested that the elements release would be strongly differentiated with reference to (i) the nature of the elements, (ii) the stage of weathering, or (iii) both of them.

From such hypothesis, the present paper aims at providing a qualitative/kinetic interpretation of the elements release processes. In particular, attention is focused on:

- finding kinetic models best fitting the observed, complex elements release;
- identifying the mineral phases involved, step by step, on elements release, with special reference to potassium taking into account its already mentioned importance as plant nutrient (*vide supra*).

2. Materials and Methods

2.1. Previous Phlegraean Yellow Tuff (PYT) Weathering Experiment

The Phlegraean Yellow Tuff (PYT) weathering experiment was widely detailed in a previous paper [30]. Here, we briefly summarize the adopted protocol.

The zeolitic-rich tuff used is the yellow facies of the Campanian Ignimbrite formation (39.000 years b.p., [33] outcropping within the Phlegraean Fields, that we have chosen to name Phlegraean Yellow Tuff. It had the following chemical composition (wt %): $SiO_2 = 54.46$, $TiO_2 = 0.43$, $Al_2O_3 = 13.96$, $Fe_2O_3 = 3.56$, $MnO = 0.13$, $MgO = 1.12$, $CaO = 4.56$, $K_2O = 6.63$, $Na_2O = 1.31$, $P_2O_5 = 0.11$, $H_2O = 13.73$, and a total zeolite content equal to 47% (30% phillipsite, 17% chabazite). Other tuff components were feldspars 39%, amorphous phases 13%, and biotite 1%. CEC was 2.12 mmol$_c$ g^{-1}.

The weathering solutions used for dissolution experiments were deionized water (W) and TA solutions at different concentrations, i.e. 3×10^1, 3×10^2, 1×10^3, 3×10^3, 1×10^4, 3×10^4 μmol·L^{-1}.

The weathering of PYT was carried out by "discontinuous equilibrium" batch through 23 weathering treatment cycles (WTCs) (each lasting seven days) to simulate natural soil saturation/leaching cycles. Five grams of PYT were placed in polypropylene tubes with 100 mL weathering solutions at room temperature and end-over-end shaken at 60 opm for the entire duration of the experiment (196 days). After each WTC supernatants were carefully removed and quantitatively replaced by fresh weathering solutions. Ca, Mg, K, Na, Fe, Al, and Si were chosen because of their relevance in pedogenic processes. The element contents were determined by flame atomic absorption spectroscopy using a Perkin-Elmer Analyst 100 Spectrometer (Waltham, MA, USA).

2.2. Kinetic Models

Sparks [32] thoroughly revised the kinetic models to understand the mechanisms of soil chemical reactions. According to the specific aim of the present paper, the following three equations were initially tested for their suitability in modeling the element release during the whole period of weathering—power function, the Weber–Morris model, and the Elovich equation.

The power function is an empirical equation given by

$$Y = k\, t^n \tag{1}$$

where Y is the concentration (mmol L^{-1}) of each element in the solution at time t, whereas k (mmol L^{-1} days^{-n}) and n (dimensionless) are constants. Equation (1) has been commonly used in the past for describing the kinetics of plant nutrient release from natural materials [34,35], as well as for kinetics of minerals dissolution [36,37]. The power function has the practical advantage over other kinetic models, such as the pseudo-second order equation [38], in that it can be applied for modelling experimental conditions far from equilibrium. The higher the values of k and n, the greater is the element release rate with time. In addition, n gives information on how the release rate varies during the weathering period; as time goes on, the release rate of each element decreases ($n < 1$, remains constant ($n = 1$) or increases ($n > 1$), respectively. For the case where $n = 0.5$, Equation (1) is similar to the parabolic diffusion equation.

The Weber–Morris model [39] can be properly used when the rate of transport of the mineral components to the reactive surface sites limits the overall reaction rate [40]. If that is the case, the dissolution process is said to be diffusion controlled and the element release can be expressed as

$$Y = k_d\, \sqrt{t} + \kappa \tag{2}$$

where k_d (mmol L^{-1} days$^{-0.5}$) is a diffusion kinetic constant and κ (mmol L^{-1}) is a constant proportional to the thickness of the boundary layer [41]. Besides adsorption studies [42–44], the equation has been used in several minerals weathering studies to describe, for example, potassium release from phlogopite [45]; dissolution of magnesium silicates [46]; and dissolution of brucite, antigorite, and talc [47].

The Elovich equation has the following form:

$$Y = 1/a \ln(a\, b) + 1/a \ln(t) \tag{3}$$

where a (L mmol^{-1}) and b (mmol L^{-1} days^{-1}) are constant.

The Elovich equation, originally developed for gas adsorption [48], has also been used for modelling minerals dissolution. Some examples are the dissolution of phosphate rocks in acidic sandy soils [49] and of zinc silicate in ammoniacal solution [50].

As discussed below (*vide infra*), the preliminary step of the present investigation is the choice of the equation best fitting, element by element, the experimental data, with specific reference to the whole 161-days release process, and/or to each of the three stages in which the release process has been subdivided.

The second step aims at assessing whether the parameters of the kinetic model describing the release of a given element change from stage to stage.

The third step is the comparative analysis and interpretation of the kinetic releases of the different elements, from the perspective of assessing the involvement of different mineral phases present in the native rock.

3. Results

3.1. Kinetic Modelling

As mentioned above (*vide supra*), the weathering of PYT was directly depending on TA concentration and that the overall elements release exhibited three distinctive stages. By way of example, Figures 1 and 2 show (i) the amount of Ca (mmol·L^{-1} vs. time) extracted by W and by TA solutions and (ii) the proton activity budget, respectively. In particular, solutions with similar tannic acid concentration behaved in an almost similar way, exhibiting analogous weathering efficiency. On the bases of such considerations, in the present paper, we will take into the account the element release in the following weathering solutions: W and TA 3×10^2, 3×10^3 and 3×10^4 µmol·L^{-1}.
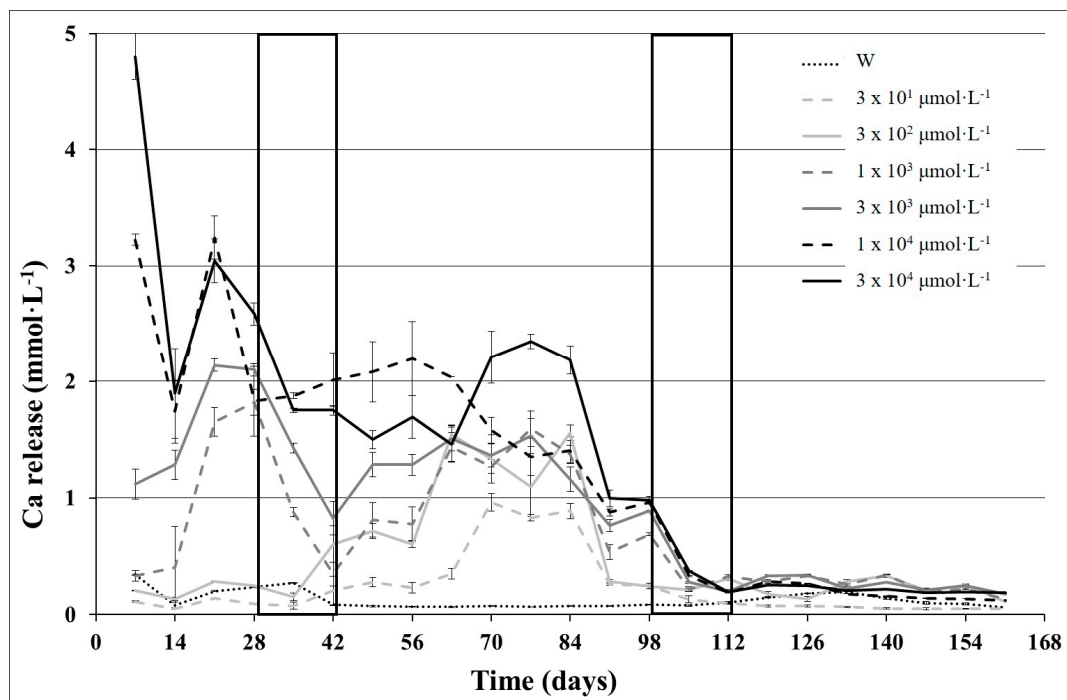
Figure 1. Amounts of Ca (mmol·L^{-1}) extracted by water (W) and tannic acid (TA) solutions versus time (days). Bars on experimental data indicate standard errors; rectangular boxes delimitate crucial steps during the experimental weathering (adapted from Grilli et al. [30]).
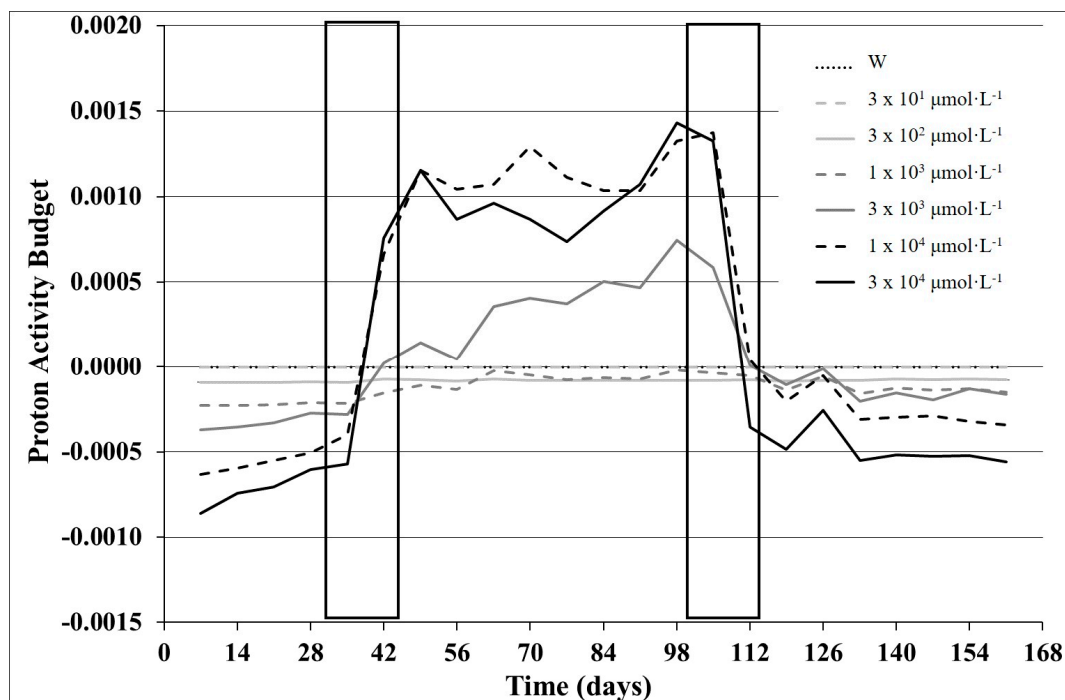
Figure 2. Proton activity budget in water (W) and tannic acid (TA) supernatants versus time (days). Rectangular boxes delimitate crucial steps during the experimental weathering (adapted from Grilli et al. [30]).

The release rate of each element during the whole experiment (161 days) has been fitted, time by time, by the three models considered in the present work; Table 1 shows the respective χ^2 and coefficient of determination (R^2).

It is evident that the power function fits the elements release very well, independently from tannic acid concentration and always showing the largest R^2 and the smallest χ^2. Therefore, the power function has been chosen as the equation modeling the release rate of each element during the three distinct stages. In particular, the three distinct temporal stages of weathering, have been more accurately identified, with respect the previous work (Figures 1 and 2)—the first stage from the beginning to 49th day; the second stage up the 98th day, and the third stage until the end of experiment (161st day). Table 2 shows the power function parameters, including the equation coefficient *k* and *n*, calculated in the three weathering stages.

It can be noted that the *k* and the *n* parameters widely vary according to (i) the nature of the element, (ii) the tannic acid concentration in extractant solution, and (iii) the specific release stage to which the equation is fitted. In fact, the *k* parameter is almost less than 1 for each stage, with a few exceptions, the most appreciable of which is represented by calcium release in TA solution during the late stage. However, as explained in the Material and Methods section, the *k* parameter has no influence on the effective trend of the release. This, in turn, is substantially conditioned by the *n* parameter, which tunes the slope of the fitting curve. In this regard, the calculated *n* values usually are less than 1, with relevant exceptions for all considered elements, in particular during the early and middle stages. Such a variability deserves detailed case-by-case discussion.

Table 1. Modelling the full data set of the elements release from Phlegraean Yellow Tuff (PYT) during the whole of weathering experiment (161 days). Goodness of fit using different kinetic equations.

Kinetic Model	TA (µmol L^{-1})	Element	χ^2	R^2	Element	χ^2	R^2	Element	χ^2	R^2
Power function	0	Si	5.68	0.969	K	0.06	0.999	Na	0.01	0.999
	3×10^2		13.19	0.985		0.15	0.997		0.34	0.980
	3×10^3		96.40	0.967		0.19	0.999		0.17	0.994
	3×10^4		79.81	0.992		18.61	0.987		0.03	0.999
Weber–Morris equation	0	Si	4.04	0.978	K	1.76	0.973	Na	0.15	0.980
	3×10^2		61.37	0.931		0.35	0.994		0.22	0.987
	3×10^3		318.88	0.891		2.8	0.980		0.14	0.995
	3×10^4		695.75	0.934		66.9	0.952		0.85	0.970
Elovich equation	0	Si	19.27	0.894	K	8.86	0.865	Na	0.92	0.884
	3×10^2		177.67	0.802		4.14	0.926		0.99	0.943
	3×10^3		768.35	0.737		16.39	0.881		1.59	0.940
	3×10^4		2113.4	0.799		245.41	0.826		3.97	0.860
Power function	0	Al	0.76	0.973	Fe	<0.01	0.780	Ca	0.29	0.976
	3×10^2		1.22	0.978		0.05	0.918		28.78	0.922
	3×10^3		19.80	0.968		0.40	0.983		40.17	0.955
	3×10^4		68.84	0.989		1.75	0.986		74.96	0.955
Weber–Morris equation	0	Al	0.85	0.97	Fe	<0.01	0.766	Ca	0.45	0.963
	3×10^2		1.21	0.978		0.01	0.978		24.57	0.933
	3×10^3		68.38	0.891		0.17	0.993		25.19	0.972
	3×10^4		198.58	0.968		0.80	0.994		66.56	0.960
Elovich equation	0	Al	0.43	0.985	Fe	<0.01	0.781	Ca	1.49	0.878
	3×10^2		3.04	0.946		0.04	0.934		57.44	0.845
	3×10^3		165.83	0.735		0.70	0.970		37.38	0.959
	3×10^4		881.94	0.857		4.97	0.960		77.48	0.953

Table 1. *Cont.*

Kinetic Model	TA (µmol L^{-1})	Element	χ^2	R^2	Element	χ^2	R^2	Element	χ^2	R^2
Power function	0	Mg	0.03	0.968						
	3×10^2		0.02	0.983						
	3×10^3		0.05	0.992						
	3×10^4		0.08	0.997						
Weber–Morris equation	0	Mg	0.03	0.969						
	3×10^2		0.08	0.94						
	3×10^3		0.02	0.997						
	3×10^4		0.31	0.987						
Elovich equation	0	Mg	0.05	0.938						
	3×10^2		0.24	0.819						
	3×10^3		0.41	0.939						
	3×10^4		2.27	0.902						

Table 2. Power function parameters calculated for each element during the three distinct weathering stages.

Element	TA (μmol L^{-1})	First Weathering Stage (0–49 Days)				Middle Weathering Stage (49–98 Days)				Late Weathering Stage (98–161 Days)			
		k	*n*	χ^2	R^2	*k*	*n*	χ^2	R^2	*k*	*n*	χ^2	R^2
Si	0	1.01	0.47	0.06	0.995	0.70	0.55	0.02	0.996	0.25	0.78	0.09	0.991
	3×10^2	0.36	0.81	0.12	0.984	0.04	**1.27**	7.14	0.898	0.09	**1.08**	0.59	0.991
	3×10^3	0.97	0.55	0.12	0.988	0.03	**1.38**	3.24	0.981	0.05	**1.29**	0.23	0.999
	3×10^4	0.52	0.89	0.71	0.988	0.06	**1.42**	4.63	0.994	0.58	0.94	5.37	0.989
Al	0	0.24	0.66	0.09	0.983	0.82	0.35	<0.01	0.998	1.02	0.31	0.01	0.982
	3×10^2	0.36	0.64	0.36	0.939	1.21	0.29	0.01	0.899	0.50	0.52	0.04	0.989
	3×10^3	0.56	0.45	0.03	0.979	0.07	**1.02**	0.06	0.978	0.09	**1.02**	4.28	0.955
	3×10^4	0.08	**1.41**	1.77	0.975	0.16	**1.15**	0.52	0.991	0.41	0.96	10.51	0.989
Mg	0	0.01	**1.04**	<0.01	0.994	0.15	0.28	<0.01	0.987	0.01	0.79	<0.01	0.973
	3×10^2	0.02	0.72	<0.01	0.991	0.005	**0.98**	<0.01	0.998	0.01	0.86	<0.01	0.989
	3×10^3	0.02	**1.00**	<0.01	0.999	0.04	0.79	<0.01	0.998	0.12	0.54	<0.01	0.987
	3×10^4	0.08	0.78	<0.01	0.998	0.11	0.68	<0.01	0.996	0.15	0.64	0.08	0.806
K	0	0.10	0.73	0.01	0.985	0.07	0.85	<0.01	0.999	0.04	0.97	0.01	0.997
	3×10^2	0.08	0.92	<0.01	0.998	0.34	0.52	<0.01	0.995	0.14	0.73	0.02	0.997
	3×10^3	0.15	0.80	<0.01	0.999	0.15	0.78	0.01	0.995	0.16	0.79	0.01	0.999
	3×10^4	0.13	0.96	<0.01	0.999	0.03	**1.37**	<0.01	0.999	0.25	0.91	0.10	0.990
Fe	0	0.01	0.39	<0.01	0.997	0.03	0.15	<0.01	0.998	0.05	0.07	<0.01	0.898
	3×10^2	0.07	0.56	<0.01	0.929	0.17	0.26	<0.01	0.996	0.09	0.44	<0.01	0.967
	3×10^3	0.03	**1.07**	<0.01	0.999	0.11	0.73	0.01	0.985	0.21	0.57	0.01	0.953
	3×10^4	0.16	0.83	<0.01	0.999	0.20	0.78	<0.01	0.998	1.05	0.41	<0.01	0.997
Na	0	0.03	0.84	<0.01	0.999	0.04	0.78	<0.01	0.999	0.02	0.91	<0.01	0.999
	3×10^2	0.07	0.78	0.01	0.990	0.02	**1.07**	<0.01	0.998	0.39	0.40	<0.01	0.995
	3×10^3	0.14	0.67	0.02	0.984	0.04	0.94	<0.01	0.999	0.30	0.52	<0.01	0.998
	3×10^4	0.05	0.84	<0.01	0.998	0.04	0.91	<0.01	0.992	0.03	0.94	0.01	0.997
Ca	0	0.02	**1.09**	0.02	0.943	0.26	0.40	<0.01	0.997	0.02	**0.99**	0.02	0.965
	3×10^2	0.02	**1.20**	<0.01	0.988	ND *	ND *	ND *	ND *	1.37	0.41	0.04	0.995
	3×10^3	0.07	**1.38**	0.05	0.997	0.23	0.97	0.01	0.999	4.87	0.29	0.55	0.966
	3×10^4	0.63	0.88	1.95	0.940	1.12	0.70	0.24	0.991	12.50	0.18	1.22	0.923

* not determined; bold values indicate *n* values close to 1 or > 1.

3.2. Kinetic Analysis of the Three Weathering Stages

As expected, the synoptic comparison among the parameters calculated for the different elements and the relative release stages puts forward complex and distinct trends of elements release. For better analyze and understand such trends, the Figures 3–5 depict the release rate (r) of each element, calculated by the first derivative of the power function (Equation (1)) with respect to time:
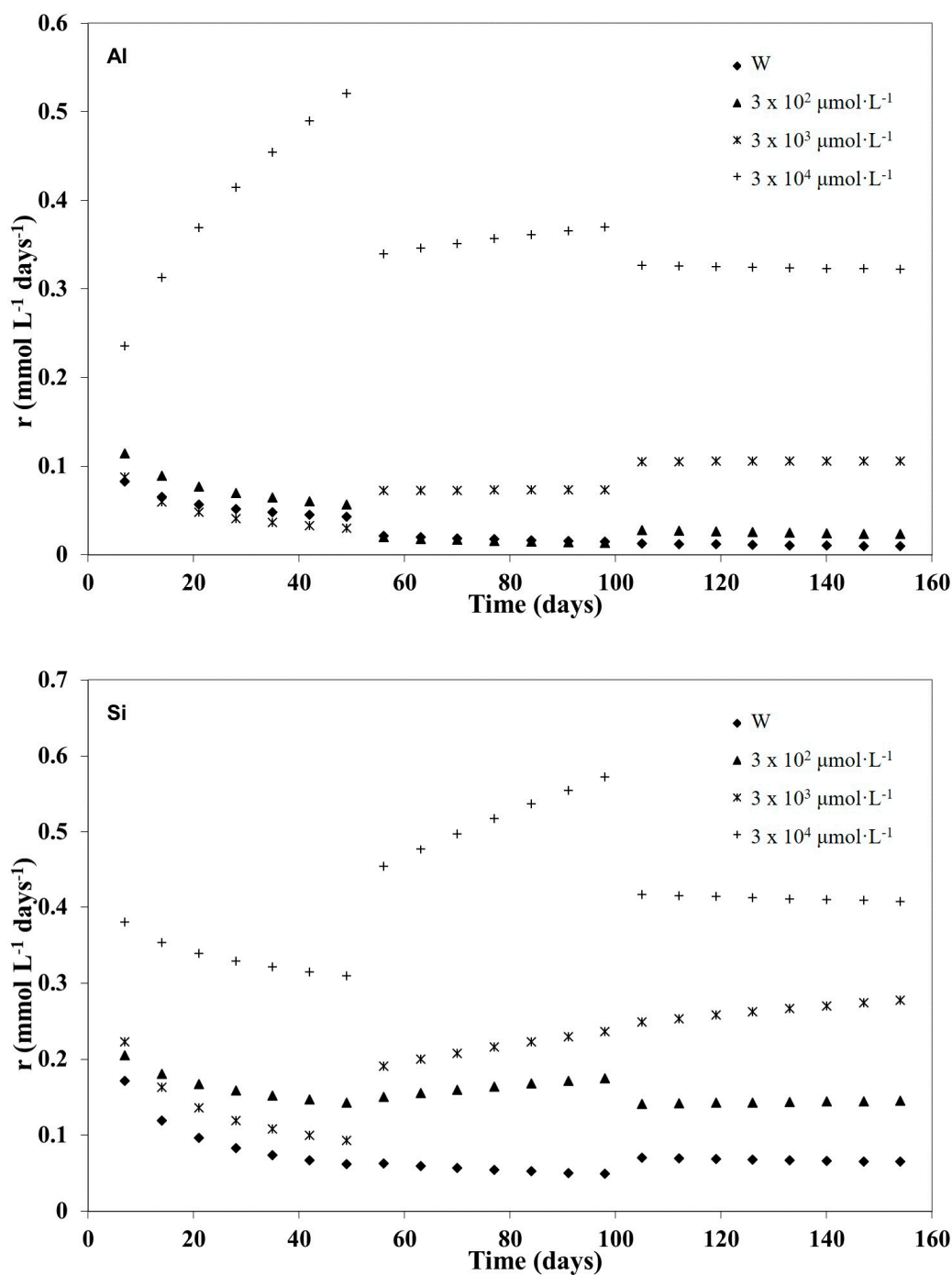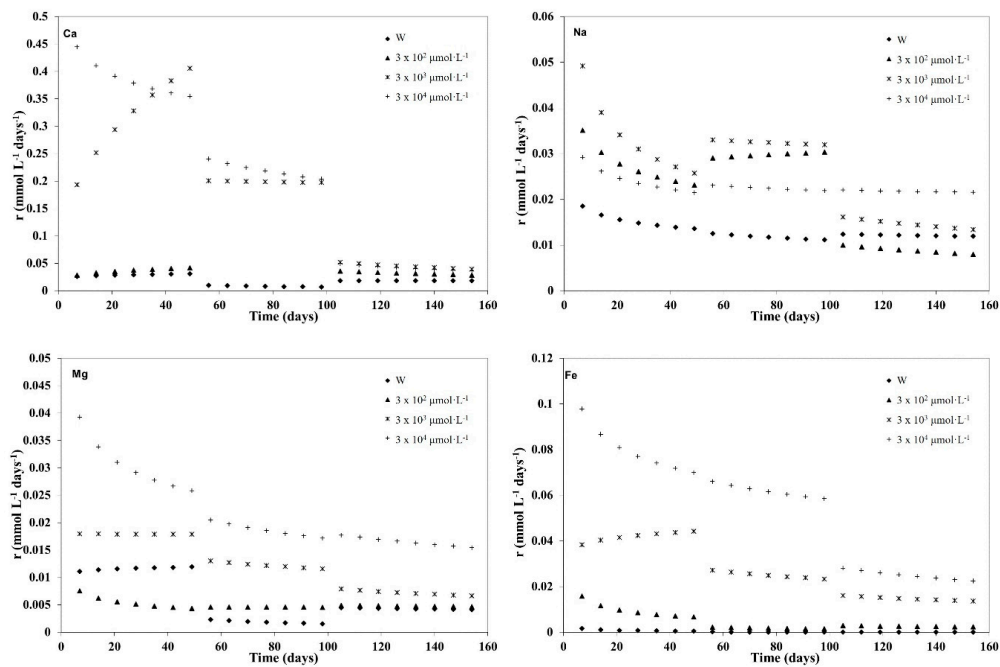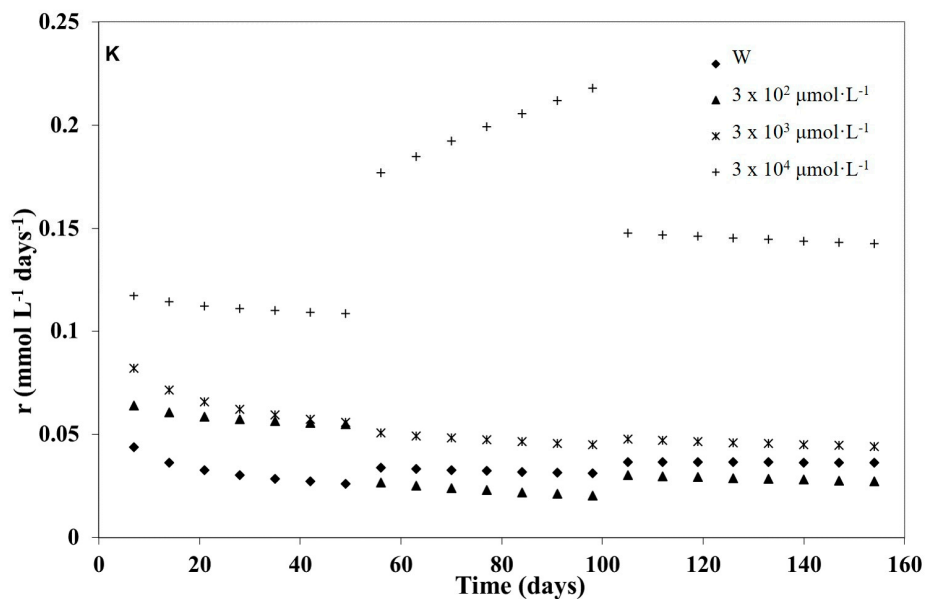
$$r = dY/dt = k\,n\,t^{n-1} \tag{4}$$

Figure 3. Release rate (r) curves of Al and Si during the three weathering stages (0–49; 49–98; 98–161 days) in water (W) and tannic acid (TA) solutions at different concentrations (3×10^2, 3×10^3 and 3×10^4 µmol·L^{-1} TA) calculated according to Equation (4).

Figure 4. Release rate (r) curves of Ca, Na, Mg, and Fe during the three weathering stages (0–49; 49–98; 98–161 days) in water (W) and tannic acid (TA) solutions at different concentrations(3×10^2, 3×10^3 and 3×10^4 μmol·L^{-1} TA), calculated according to Equation (4).

Figure 5. Release rate (r) curves of K during the three weathering stages (0–49; 49–98; 98–161 days) in water (W) and tannic acid (TA) solutions at different concentrations(3×10^2, 3×10^3 and 3×10^4 μmol·L^{-1} TA), calculated according to Equation (4).

Several aspects must be considered. It is appropriate to clarify that from now onward we assume that when extraction curves show similar trends, it likely implies that analogous physical-chemical release processes occurred and the same mineral phases are involved. In the first weathering stage, the release rates usually decrease during the extraction process, with some relevant exceptions including Al (Figure 3), Ca, Fe, and Mg (Figure 4). As a matter of fact, for these elements, the *n* parameter of the fitting equation sometime is close to or larger than 1 (Table 2), thus implying that the release rate tends to be constant, or to increase as time goes on, respectively. In this last case, the release rate curve exhibits

a "convex" shape. The "convexity" suggests a sort of "activation" of release process, which becomes more efficient as the weathering proceeds. Such an occurrence is particularly marked for Al (in TA 3×10^4 µmol·L^{-1}solution; Figure 3) and, to a lesser extent, Fe (in TA 3×10^3 µmol·L^{-1} solution; Figure 4) and Mg (in W and in TA 3×10^3 µmol·L^{-1} solution; Figure 4); for Ca, *n* increases along with TA concentration from 0 (water) to 3×10^3 µmol·L^{-1}, but is equal to 0.88 in TA 3×10^4 µmol·L^{-1} solution (Figure 4).

As a matter of fact, the tannic acid concentration does not affect in the same way the release of the different elements. Tannic acid, similar to humic acids, can interact with the tuff surface promoting the release/chelation of elements [51–53]. In the first weathering stage and in the absence of TA, the release rate of Al and K is lower than that of Ca and Na (see n values in Table 2). In contrast, at the highest concentration investigated, TA dramatically enhances the release of structural elements (especially Al), causing a partial loss of crystallinity of the tuff minerals and thus favoring the release of strongly retained exchangeable elements such as K. The charge density may have a great impact on the elements ability to be chelated by tannic acid. This is particularly evident for Na (Figure 3), which, as hydrated large monovalent cation, does not form stable chelates with tannic acid [54]. The opposite is true for Fe release (Figure 3), which is directly dependent on TA concentration, according to its well-known ability to be bound by tannic acid [55]. We must also take into account that the considered elements, or even a same element, arise from mineral phases that are either amorphous or crystalline, which in turn are differently prone to be weathered. In particular, during the first stage, it is reasonable to infer that loosely bound elements are primarily removed, such as Fe, Mg, and K prevailingly from biotite and Si, Al, Ca, and Na mainly from amorphous aluminosilicates.

The examination of the release rate during the second stage clearly highlights dramatic quali-quantitative changes in the weathering process (Figures 3–5). In fact, for each element, further changes of both rate and *n* parameter occur, compared to the first stage. The most remarkable variation is the wide gap discriminating the elements release in the solution with the largest TA concentration with respect to the lower concentration solutions.

Specifically, for both Si and Al the *n* parameter tends to increase with TA concentration of extractant solutions (Table 2), suggesting that the release of these elements is "activated" during the second stage (Figure 3), with a possible concurrent weathering of the same mineralogical phases. Such an hypothesis can be supported by a concomitant increment of *n* parameter for potassium which, in 3×10^4 µmol·L^{-1} TA solution, reaches 1.37 (Table 2). In fact, in this last extractant solution, the release trend of potassium (Figure 5) becomes more similar to those of silicon and aluminum (Figure 3), while quite differs from those of iron and magnesium. These two, in turn, still exhibit similar dissolution patterns (Figure 4). This could indicate that, during the middle stage, potassium should arise from other sources than biotite, such as zeolites. This could be corroborated by the releases observed for calcium and sodium—also present in zeolites—that show high rates, but almost constant, with smoothed slopes quite different from those detected during the first stage (Figure 4). These variations imply that the bulk of sodium and calcium is extracted during the first stage from amorphous (volcanic glass), but they continue to be released during the middle stage deriving also from crystalline phases, e.g., phillipsite and chabasite. Truly, the release rate curves of Na and Ca are distinct from the respective curves observed during the first stage (Figure 4), as well as from those of Si, Al, and K during the middle stage (Figures 3 and 5). This is consistent with the coexistence of amorphous and crystalline phases in PYT, which are variously weathered during the whole experiment [30].

During the late weathering stage, the dissolution rates calculated for the different elements tend to be less heterogeneous and more coherent (Figures 3–5). Specifically, the slopes are not as steep as in the previous stages, with *n* parameter values usually less than or close to 1. However, differences are still evident with respect to the absolute values of release rates, likely depending on the initial amount of the native elements.

For a better interpretation of the release processes during the final stage, the rates have been normalized to the amounts of the native elements. Figure 6 shows as an example the normalized

release trend observed for water (a) and maximum TA concentration (b). It is obvious that all the release rates tend to become constant, with similar order of magnitude along with the TA concentration. In other words, after normalization, the release rates in the last stage are substantially dependent from the concentration of weathering solutions and from the nature of element, rather than the respective amounts of native elements. All this clearly denotes that during the last stage the weathering of every mineral phase proceeds slowly but steadily towars the definitive breakdown and transformation of the parent material. After the end of the WTC experiments (161 days), the weathering process carried out in the presence of the highest TA concentration (3×10^4 µmol·L^{-1}) leads to a decrease in the PYT zeolites content of 73.3% (phillipsite) and of 41.1% (chabazite), accompanied by a total mass loss of 26.3%.
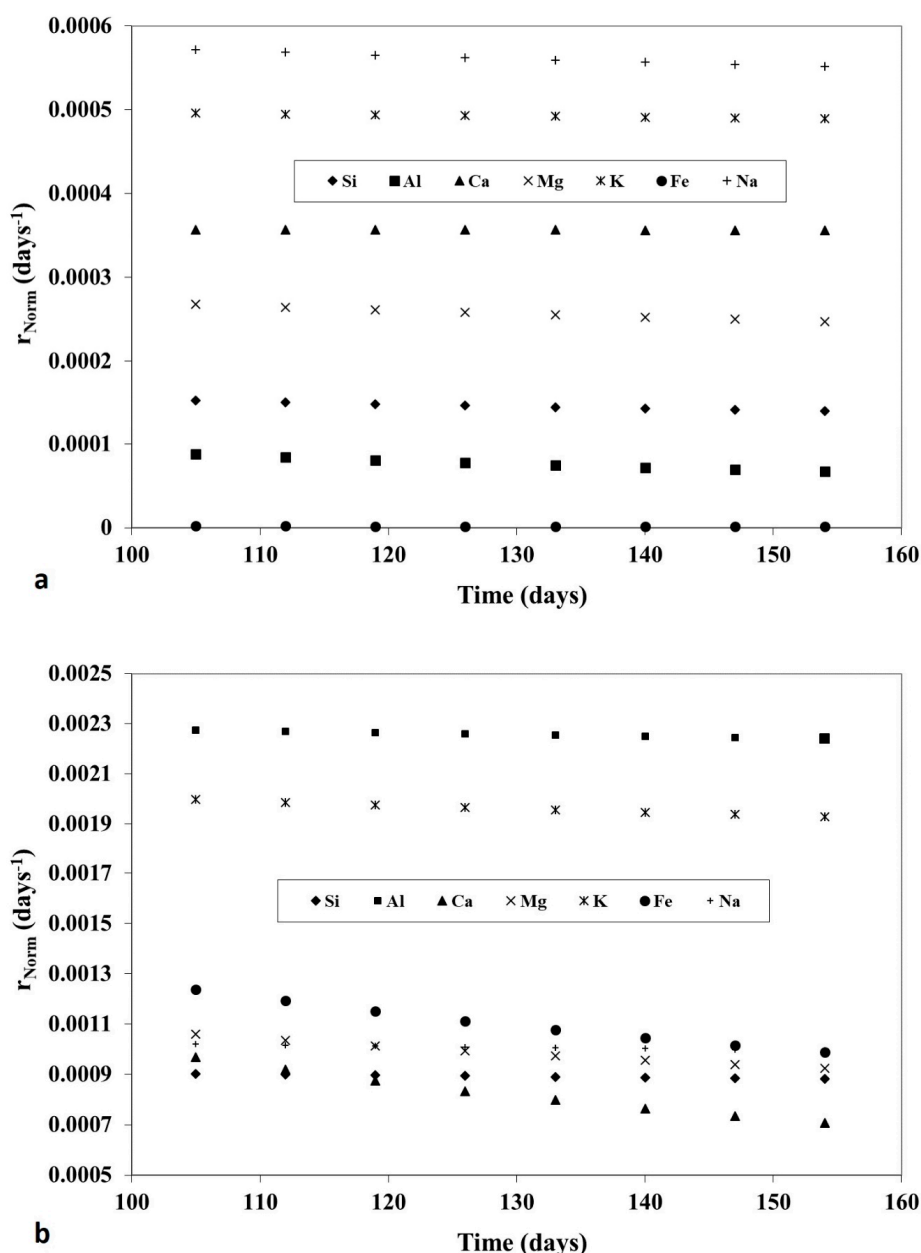
Figure 6. Normalized release rate (rNorm) curves of Si, Al, Ca, Mg, K, Fe, and Na during the late stage of the weathering process (98–161 days), in water (**a**) and tannic acid (**b**) solution at maximum concentration (3×10^4 µmol·L^{-1} TA).

4. Conclusions

The outcomes of the present investigation inspire several remarks.

From the kinetic modelling standpoint, the power function was revealed to be an excellent empirical equation fitting the experimental elements releases, which are clearly characterized by huge differences in qualitative and quantitative terms. This allowed us to gain numerical parameters that, even if empirical, are in any case suitable predictive tools. Specifically, the variability of *n* parameter has been consistently related to actual chemical-physical factors such as the concentration of tannic acid solutions or the nature of the considered elements. Furthermore, the huge variability of *n* directly focused the attention on the various (and sometimes dramatically divergent) release trends observed in the different weathering stages, thus highlighting the intensity of the weathering and the modality of element release. In turn, this accounted for the involvement of distinct mineral phases during the experiment.

By paralleling the dissolution rates of each element during the three stages, it is possible to guess the various sources from which they are released. During the first stage, Fe, Mg, and K likely arise from biotite, Ca and Na from amorphous, and Al and Si from both of them. The second stage denotes, concurrently to amorphous weathering, the early breakdown of zeolite framework, from which Al, Si, Ca, Na, and K are further released. In the third stage, the whole of weathering/release process approaches a steady state. The outcomes of the present investigation are also remarkable and convenient to forecast the behavior of pedogenic and nutritional potential of zeolitic-rich tuffs when utilized as pedotechnical matrices in restoration design.

References

1. Aainaa, H.N.; Ahmed, O.H.; Majid, N.M.A. Effects of clinoptilolite zeolite on phosphorus dynamics and yield of *Zea Mays* L. cultivated on an acid soil. *PLoS ONE* **2018**, *13*, e0204401. [CrossRef]

2. Ming, D.W.; Allen, E.R. Use of natural zeolites in agronomy, horticulture, and environmental soil remediation. *Rev. Mineral. Geochem.* **2001**, *45*, 618–654. [CrossRef]

3. Doula, M.K.; Kavvadias, V.A.; Elaiopoulos, K. Zeolites in soil remediation processes. In *Handbook of Natural Zeolites*; Bentham Science Publishers: Sharjah, UAE, 2012; pp. 519–568.

4. Hamidpour, M.; Shariatmadari, H.; Soleimani, M. Zeoponic systems. In *Handbook of Natural Zeolites*; Bentham Science Publishers: Sharjah, UAE, 2012; pp. 588–600.

5. Margeta, K.; Zabukovec, N.; Siljeg, M.; Farkas, A. Natural Zeolites in Water Treatment—How Effective is Their Use. In *Water Treatment*; InTechOpen Ltd.: London, UK, 2013.

6. Filcheva, E.; Chakalov, K. Soil fertility management with zeolite amendments. i. effect of zeolite on carbon sequestration: A review. In *Agricultural Practices and Policies for Carbon Sequestration in Soil*; CRC Press: Boca Raton, FL, USA, 2016; pp. 223–228.

7. Soudejani, H.T.; Kazemian, H.; Inglezakis, V.J.; Zorpas, A.A. Application of zeolites in organic waste composting: A review. *Biocatal. Agric. Biotechnol.* **2019**, *22*, 101396. [CrossRef]

8. Montalvo, S.; Huiliñir, C.; Borja, R.; Sánchez, E.; Herrmann, C. Application of zeolites for biological treatment processes of solid wastes and wastewaters—A review. *Bioresour. Technol.* **2020**, *301*. [CrossRef] [PubMed]

9. Salvestrini, S.; Vanore, P.; Iovino, P.; Leone, V.; Capasso, S. Adsorption of simazine and boscalid onto acid-activated natural clinoptilolite. *Environ. Eng. Manag. J.* **2015**, *14*, 1705–1712. [CrossRef]

10. Gkotsis, P.; Peleka, E.; Zouboulis, A. The Use of Natural Minerals in a Pilot-Scale MBR for Membrane Fouling Mitigation. *Separations* **2020**, *7*, 24. [CrossRef]

11. Vera-Puerto, I.; Saravia, M.; Olave, J.; Arias, C.; Alarcon, E.; Valdes, H. Potential Application of Chilean Natural Zeolite as a Support Medium in Treatment Wetlands for Removing Ammonium and Phosphate from Wastewater. *Water* **2020**, *12*, 1156. [CrossRef]

12. Salvestrini, S.; Sagliano, P.; Iovino, P.; Capasso, S.; Colella, C. Atrazine adsorption by acid-activated zeolite-rich tuffs. *Appl. Clay Sci.* **2010**, *49*, 330–335. [CrossRef]

13. Leone, V.; Canzano, S.; Iovino, P.; Salvestrini, S.; Capasso, S. A novel organo-zeolite adduct for environmental applications: Sorption of phenol. *Chemosphere* **2013**, *91*, 415–420. [CrossRef]

14. Kuntubek, A.; Kinayat, N.; Meiramkulova, K.; Poulopoulos, S.; Bear, J.C.; Inglezakis, V.J. Catalytic Oxidation of Methylene Blue by Use of Natural Zeolite-Based Silver and Magnetite Nanocomposites. *Processes* **2020**, *8*, 471. [CrossRef]

15. Leone, V.; Iovino, P.; Salvestrini, S.; Capasso, S. Sorption of non-ionic organic pollutants onto a humic acids-zeolitic tuff adduct: Thermodynamic aspects. *Chemosphere* **2014**, *95*, 75–80. [CrossRef]

16. Naumova, L.; Gorlenko, N.; Kurzina, I. Photocatalytic Activity of the Iron-Containing Natural Composites in the Reaction of Oxidative Destruction of Oxalic Acid and Phenol. *Environments* **2018**, *5*, 16. [CrossRef]

17. Buondonno, A.; Coppola, E.; Bucci, M.; Battaglia, G.; Colella, A.; Langella, A.; Colella, C. Zeolitized tuffs as pedogenic substrate for soil re-building. Early evolution of zeolite/organic matter proto-horizons. *Stud. Surf. Sci. Catal.* **2002**, *142*, 1751–1758.

18. Buondonno, A.; Colella, A.; Coppola, E.; de Gennaro, B.; de' Gennaro, M.; Gargiulo, N.; Langella, A.; Leone, A.P.; Letizia, A.; Rubino, M.; et al. Properties of zeolitized tuff/organic matter aggregates relevant for their use in pedotechnique. III: Organic matter stability and exchange properties. *Stud. Surf. Sci. Catal.* **2007**, *170*, 2141–2146.

19. Buondonno, A.; Colella, A.; Coppola, E.; de Gennaro, B.; Gargiulo, N.; Langella, A.; Letizia, A.; Colella, C. Properties of zeolitized tuff/organic matter aggregates relevant for their use in pedotechnique. IIb: Structural characterization with emphasis on surface and porosity properties. *Stud. Surf. Sci. Catal.* **2008**, *174*, 517–520. [CrossRef]

20. Buondonno, A.; Grilli, E.; Capra, G.F.; Glorioso, C.; Langella, A.; Leone, A.P.; Leone, N.; Odierna, P.; Vacca, S.; Vigliotti, R.C. Zeolitized tuffs in pedotechnique for the reclamation of abandoned quarries. A case study in the Campania region (Italy). *J. Environ. Manage.* **2013**, *122*, 25–30. [CrossRef] [PubMed]

21. Bucci, M.; Buondonno, A.; Colella, C.; Coppola, E.; Leone, A.P.; Mammucari, M. Properties of zeolitized tuff/organic matter aggregates relevant for their use in pedotechnique I. Chemical and physical-chemical properties. *Stud. Surf. Sci. Catal.* **2005**, *155*, 103–116.

22. De Gennaro, B.; Aprea, P.; Colella, C.; Buondonno, A. Comparative ion-exchange characterization of zeolitic and clayey materials for pedotechnical applications-Part 1: Interaction with noxious cations. *J. Porous Mater.* **2007**, *14*, 349–356. [CrossRef]

23. De Gennaro, B.; Aprea, P.; Colella, C.; Buondonno, A. Comparative ion-exchange characterization of zeolitic and clayey materials for pedotechnical applications—Part 2: Interaction with nutrient cations. *J. Porous Mater.* **2009**, *16*, 667–673. [CrossRef]

24. Capra, G.F.; Buondonno, A.; Coppola, E.; Duras, M.G.; Vacca, S.; Colella, C. Zeolitized tuffs in pedotechniques to improve soil resilience against the impact of treatment by municipal sewage: Balance of nutrient and noxious cations. *Clay Miner.* **2011**, *46*, 261–278. [CrossRef]

25. Capra, G.F.; Duras, M.G.; Vacca, S.; Grilli, E.; Buondonno, A. Issues concerning soils treated with wastewater: Pedotechnical management with zeolitized tuffs as an option for turning N and P pollutants into potential fertilizers. *Microporous Mesoporous Mater.* **2013**, *167*, 22–29. [CrossRef]

26. Capra, G.F.; Grilli, E.; Macci, C.; Vacca, S.; Masciandaro, G.; Ceccanti, B.; Bondi, G.; Duras, M.G.; Dessena, M.A.; Marras, G.; et al. Lake-dredged material (LDM) in pedotechnique for the restoration of Mediterranean soils affected by erosion/entisolization processes. *J. Soils Sediments* **2014**, *15*, 32–46. [CrossRef]

27. Wilson, G.; van Ouwerkerk, C. Pedotechnique, the link between pedology and engineering. *Soil Tillage Res.* **1987**, *10*, 1–3. [CrossRef]

28. Koolen, A.J.; Rossignol, J.P. Introduction to symposium 19: Construction and use of artificial soils. *Soil Tillage Res.* **1998**, *47*, 151–155.

29. Ming, D.W.; Boettinger, J.L. Zeolites in Soil Environments. *Rev. Mineral. Geochem.* **2018**, *45*, 323–346. [CrossRef]

30. Grilli, E.; Colella, A.; Coppola, E.; Langella, A.; Buondonno, A. Modelling pedogenization of zeolitized tuff: Effects of water and phenolic substances on weathering rates of the Campanian Ignimbrite (yellow facies). *Clay Miner.* **2011**, *46*, 311–327. [CrossRef]

31. Buondonno, A.; Colella, A.; Colella, C.; Coppola, E.; de' Gennaro, B.; de' Gennaro, M.; Gargiulo, N.; Grilli, E.; Langella, A.; Rubino, M. Modeling pedogenization of zeolitized tuffs. II: Medium-term weathering of phlegraean yellow tuff and red tuff with black scoriae by water and humic acids. *Stud. Surf. Sci. Catal.* **2007**, *170*, 2092–2097.

32. Robarge, W.P. Precipitation/dissolution reactions in soils. In *Soil Physical Chemistry*, 2nd ed.; CRC Press: Boca Raton, FL, USA, 2018; pp. 193–238.

33. De Vivo, B.; Rolandi, G.; Gans, P.B.; Calvert, A.; Bohrson, W.A.; Spera, F.J.; Belkin, H.E. New constraints on the pyroclastic eruptive history of the Campanian volcanic Plain (Italy). *Mineral. Petrol.* **2001**, *73*, 47–65. [CrossRef]

34. Kuo, S.; Lotse, E.G. Kinetics of Phosphate Adsorption and Desorption By Lake Sediments. *Soil Sci. Soc. Am. J.* **1974**, *38*, 50–54. [CrossRef]

35. Havlin, J.L.; Westfall, D.G. Potassium Release Kinetics and Plant Response in Calcareous Soils. *Soil Sci. Soc. Am. J.* **1985**, *49*, 366–370. [CrossRef]

36. Zhang, H.; Bloom, P.R. Dissolution Kinetics of Hornblende in Organic Acid Solutions. *Soil Sci. Soc. Am. J.* **1999**, *63*, 815–822. [CrossRef]

37. Acosta-Vigil, A.; London, D.; Dewers, T.A.; Morgan VI, G.B. Dissolution of corundum and andalusite in H2O-saturated haplogranitic melts at 800 °C and 200 MPa: Constraints on diffusivities and the generation of peraluminous melts. *J. Petrol.* **2002**, *43*, 1885–1908. [CrossRef]

38. Canzano, S.; Iovino, P.; Leone, V.; Salvestrini, S.; Capasso, S. Use and misuse of sorption kinetic data: A common mistake that should be avoided. *Adsorpt. Sci. Technol.* **2012**, *30*, 217–225. [CrossRef]

39. Weber, W. Kinetics of Adsorption on Carbon from Solution. *J. Sanit. Eng. Div.* **1963**, *89*, 31–60.

40. Salvestrini, S.; Vanore, P.; Bogush, A.; Mayadevi, S.; Campos, L.C. Sorption of metaldehyde using granular activated carbon. *J. Water Reuse Desalin.* **2017**, *7*, 280–287. [CrossRef]

41. Gupta, G.S.; Prasad, G.; Singh, V.N. Removal of chrome dye from carpet effluents using coal-ii (rate processes). *Environ. Technol. Lett.* **1988**, *9*, 1413–1422. [CrossRef]

42. Cheknane, B.; Zermane, F.; Baudu, M.; Bouras, O.; Basly, J.P. Sorption of basic dyes onto granulated pillared clays: Thermodynamic and kinetic studies. *J. Colloid Interface Sci.* **2012**, *381*, 158–163. [CrossRef]

43. Salvestrini, S.; Canzano, S.; Iovino, P.; Leone, V.; Capasso, S. Modelling the biphasic sorption of simazine, imidacloprid, and boscalid in water/soil systems. *J. Environ. Sci. Heal. B Pestic. Food Contam. Agric. Wastes* **2014**, *49*, 578–590. [CrossRef]

44. Chianese, S.; Fenti, A.; Iovino, P.; Musmarra, D.; Salvestrini, S. Sorption of organic pollutants by humic acids: A review. *Molecules* **2020**, *25*, 918. [CrossRef]

45. Da Silva, A.D.A.S.; Sampaio, J.A.; Da Luz, A.B.; França, S.C.A.; Ronconi, C.M. Modeling controlled potassium release from phlogopite in solution: Exploring the viability of using crushed phlogopitite rock as an alternative potassium source in Brazilian soil. *J. Braz. Chem. Soc.* **2013**, *24*, 1366–1372. [CrossRef]

46. Luce, R.W.; Bartlett, R.W.; Parks, G.A. Dissolution kinetics of magnesium silicates. *Geochim. Cosmochim. Acta* **1972**, *36*, 35–50. [CrossRef]

47. Lin, F.C.; Clemency, C.V. The dissolution kinetics of brucite, antigorite, talc, and phlogopite at room temperature and pressure. *Am. Mineral.* **1981**, *66*, 801–806.

48. Freund, T. Diffusion and gas sorption rates obeying the elovich equation. *J. Chem. Phys.* **1957**, *26*, 713. [CrossRef]

49. He, Z.L.; Yao, H.; Calvert, D.V.; Stoffella, P.J.; Yang, X.E.; Chen, G.; Lloyd, G.M. Dissolution characteristics of central Florida phosphate rock in an acidic sandy soil. *Plant Soil* **2005**, *273*, 157–166. [CrossRef]

50. Ding, Z.; Yin, Z.; Hu, H.; Chen, Q. Dissolution kinetics of zinc silicate (hemimorphite) in ammoniacal solution. *Hydrometallurgy* **2010**, *104*, 201–206. [CrossRef]

51. Salvestrini, S. New insights into the interaction mechanism of humic acids with phillipsite. *React. Kinet. Mech. Catal.* **2017**, *120*, 735–752. [CrossRef]

52. Colella, A.; de Gennaro, B.; Salvestrini, S.; Colella, C. Surface interaction of humic acids with natural and synthetic phillipsite. *J. Porous Mater.* **2015**, *22*, 501–509. [CrossRef]

53. Lin, J.; Zhan, Y.; Zhu, Z.; Xing, Y. Adsorption of tannic acid from aqueous solution onto surfactant-modified zeolite. *J. Hazard. Mater.* **2011**, *193*, 102–111. [CrossRef]

54. Iglesias, J.; García de Saldaña, E.; Jaén, J.A. On the tannic acid interaction with metallic iron. *Hyperfine Interact.* **2001**, *134*, 109–114. [CrossRef]

55. Iffat, A.T.; Maqsood, Z.T.; Fatima, N. Study of complex formation of Fe(III) with tannic acid. *J. Chem. Soc. Pakistan* **2005**, *27*, 174–177.